CALPHAD: Computer Coupling of Phase Diagrams and Thermochemistry 47 (2014) 129–135

Contents lists available at ScienceDirect

CALPHAD: Computer Coupling of Phase Diagrams and Thermochemistry

journal homepage: www.elsevier.com/locate/calphad

Thermodynamic assessment of the Sb–Sm and Sm–Sn systems

X.J. Liu [a,b], M.H. Chen [a], Y. Lu [a,b], Y.X. Huang [a,b], D. Wang [a], Q. He [a], D.L. Zhao [c], C.P. Wang [a,b,*]

[a] *Department of Materials Science and Engineering, College of Materials, Xiamen University, Xiamen 361005, PR China*
[b] *Research Center of Materials Design and Applications, Xiamen University, Xiamen 361005, PR China*
[c] *Beijing General Iron and Steel Research Institute, Beijing 100081, China*

ARTICLE INFO

Article history:
Received 26 March 2014
Received in revised form
25 July 2014
Accepted 25 July 2014
Available online 10 August 2014

Keywords:
CALPHAD method
Rare earth alloys
Thermodynamic calculation

ABSTRACT

The thermodynamic assessment of the Sb–Sm and Sm–Sn binary systems have been carried out by using the CALPHAD (CALculation of PHAse Diagrams) method on the basis of the experimental data including phase equilibria and thermodynamic properties. The Gibbs free energies of the solution phases (Liquid, Bcc, Bct, Hcp and Rhombohedral phase) were described by the subregular solution model with the Relich–Kister polynomial, and those of the intermetallic compounds were described by the two-sublattice model. A consistent set of thermodynamic parameters has been derived for describing the Gibbs free energies of each phase in the Sb–Sm and Sm–Sn systems. A reasonable agreement was obtained between the calculated results and experimental data.

1. Introduction

The rare earth (RE) elements have gained particular attention for their favorable magnetic, optical, electric, mechanical properties and the alloys formed with rare earth metals have always found application as high-performance functional materials, such as permanent magnets, semiconductors, lead-free solder alloys and hydrogen storage materials [1–6]. By adding a small amount of rare earth elements, the mechanical properties of Mg-based alloys can be substantially improved for microstructure development [7]. It is well known that more detailed knowledge about the phase equilibria and thermodynamic properties of rare earth alloy systems is very important to enhance the development of new rare earth material with superior properties. In order to construct a primary thermodynamic database of phase diagram in multi-component rare earth alloy systems, the thermodynamic description of each lower-order system which forms a part of this database is necessary to carry out. A series of the thermodynamic assessment of rare earth binary systems have already been performed by our research group [8–12].

The purpose of this work is to present the thermodynamic assessment of the Sb–Sm and Sm–Sn binary systems by means of the CALPHAD method, which is a powerful tool to save cost and time during the development of new materials [13]. The thermodynamic parameters of each phase in the Sb–Sm and Sm–Sn systems are optimized by fitting the experimental data on phase equilibria and thermodynamic properties.

2. Experiment information

2.1. Sb–Sm system

Regarding to the Sb–Sm system, the information on the structure properties of the individual compounds was firstly available in the literature [14–16]. Then Borzone et al. [17] systematically investigated the properties of Sb–Sm intermetallic compounds by metallographic, X-ray analysis and differential thermal analysis (DTA). In the work of Borzone et al., the Sb–Sm system was reported to include five intermetallic phases: Sb_2Sm, Sb_3Sm_5, Sb_3Sm_4, SbSm and $SbSm_2$, and no phase diagram was proposed, but a tentative one drawn on the base of analogy with the Nd–Sb system was sketched.

Subsequently, two experimental descriptions of the phase relations in the Sb–Sm system were reported by Sadigov et al. [18] and Abulkhaev [19], respectively. The complete phase diagram of the Sb–Sm system was firstly constructed using differential thermal analysis, X-ray diffraction and microstructural analysis by Sadigov et al. [18], who confirmed four intermetallic compounds: SbSm (congruent melting at 1922 °C), Sb_2Sm, Sb_3Sm_4 and Sb_3Sm_5 (peritectic formations at 1372 °C, 1792 °C and 1732 °C, respectively). The additional existence of $SbSm_2$ compound in Ref. [17] was not found by Sadigov et al. [18]. Two eutectic reactions: $L\ (4\ at\%\ Sm) \leftrightarrow (Sb) + Sb_2Sm$ at 602 °C and $L\ (90\ at\%\ Sm) \leftrightarrow Sb_3Sm_5 + (\beta Sm)$ at 1027 °C were determined and a polymorphic

---

* Corresponding author at: Department of Materials Science and Engineering, College of Materials, Xiamen University, Xiamen 361005, PR China.
Tel.: +86 592 2180606; fax: +86 592 2187966.
E-mail address: wangcp@xmu.edu.cn (C.P. Wang).

http://dx.doi.org/10.1016/j.calphad.2014.07.002
0364-5916/© 2014 Elsevier Ltd. All rights reserved.

transformation: (βSm)↔(αSm) occurred at 734 °C was also found in the Sb–Sm system.

In 1992, Abulkhaev [19] also experimentally reinvestigated the Sb–Sm phase diagram in the whole composition region, where SbSm melted congruently at 1875 °C and Sb_2Sm, Sb_3Sm_4 and Sb_3Sm_5 formed by peritectic reactions at 900 °C, 1680 °C and 1275 °C, respectively. Two eutectic reactions: L (0.2 at% Sm)↔(Sb)+Sb_2Sm at 625 °C and L (90 at% Sm)↔Sb_3Sm_5+(γSm) at 950 °C were also determined. The polymorphic transformation of the Sb_3Sm_5 phase which appeared at 1020 °C was indentified for the first time. By comparing the phase diagrams reported by Sadigov et al. [18] and Abulkhaev [19], it can be found that these two phase diagrams significantly differ with regard to invariant temperatures. According to the comment of Abulkhaev [19], the higher temperatures of invariant reactions obtained in Ref. [18] may be caused by the oxidation of the alloys during synthesis. The phase diagram of the Sb–Sm system was reviewed by Okamoto [20], as shown in Fig. 1.

The experimental thermodynamic properties of the Sb–Sm system were reported by several authors [17,21–23]. Lebedev et al. [21] employed EMF (Electromotive forces) technique to investigate the thermodynamic characteristic of Sm in liquid Sb at infinite dilution at 1000 K. Viksman and Gordienko [22] determined the enthalpy of formation of the SbSm compound by vapor pressure measurement. In addition, the enthalpies of formation of the intermetallic compounds in the Sb–Sm system were measured by Borzone et al. [17] using a different direct isoperibol calorimetry. Colinet and Pasturel [23] also predicted the enthalpy values of the Sb–Sm intermetallic compounds with various compositions by Miedema's model.

The Sb–Sm system has been thermodynamically optimized by Cacciamani et al. [24] without considering the phase diagram newly reported by Abulkhaev [19]. In the present work, the thermodynamic assessment of the Sb–Sm system is re-optimized based on the phase diagram from Abulkhaev [19] and the related thermodynamic information.

2.2. Sm–Sn system

Using differential thermal analysis, metallographic and X-ray method, the phase diagram of the Sn–Sm binary system was investigated by Percheron [25], where the following six intermetallic phases: Sm_5Sn_3 (congruent melting at 1505 °C), $SmSn_3$ (congruent melting at 1090 °C), Sm_4Sn_3, Sm_5Sn_4, $Sm_{11}Sn_{10}$ and Sm_2Sn_3 (peritectic formations at 1440 °C, 1420 °C, 1170 °C and 1105 °C, respectively) were verified. Percheron [25] also determined three eutectic reactions: L (11 at% Sn)↔(βSm)+Sm_5Sn_3 at 906 °C, L (67 at% Sn)↔Sm_2Sn_3+$SmSn_3$ at 1080 °C and L (99.8 at% Sn)↔$SmSn_3$+(Sn) at 229 °C and a polymorphic transformation: (βSm)↔(αSm) at 916 °C. But the trend of liquidus in the composition range between Sm_5Sn_3 and $SmSn_3$ compounds was not identified by Percheron [25].

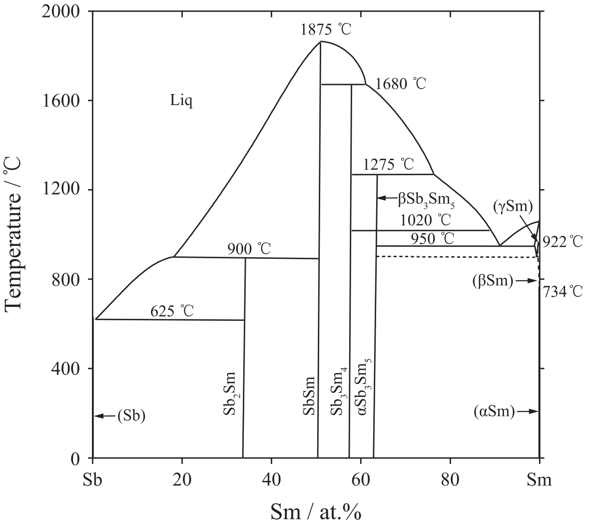

Fig. 1. The phase diagram of the Sb–Sm system reviewed by Okamoto [20].

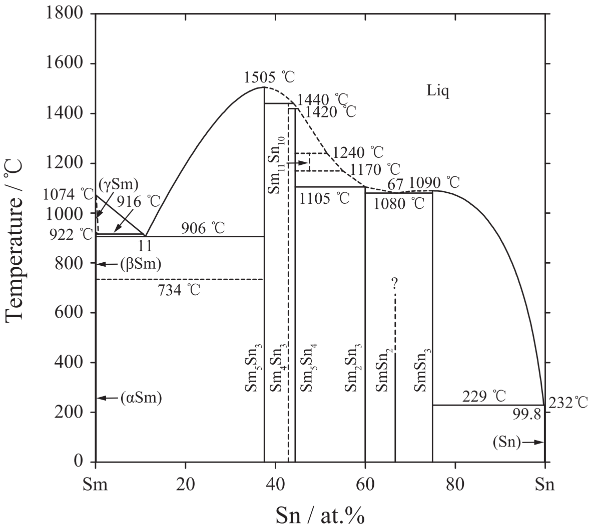

Fig. 2. The phase diagram of the Sm–Sn system drawn by Massalski [27].

Subsequently, Borzone et al. [26] briefly reviewed the phase diagram and thermodynamic information of the Sm–Sn binary system. In the work of Borzone et al. [26], the existence of $SmSn_2$ phase in the Sm–Sn system was firstly confirmed but the phase stability temperature of the $SmSn_2$ compound was not determined. During the thermodynamic optimization, the $SmSn_2$ phase as a pertectic compound was included in the Sm–Sn system. Fig. 2 shows the phase diagram of the Sm–Sn system compiled by Massalski et al. [27] according to the works mentioned above [25,26].

Peluso and Pool [28], Percheron et al. [29] and Meyer [30] measured the limiting partial enthalpies of Sm in liquid Sn at 750 K, 967.5 K and 1173 K, respectively by dissolution calorimetry at high dilution. The approximate range of the limiting partial enthalpy value at 828 K was determined by Pratt and Morris [31] using low solution rate calorimetry and a very negative value at 1000 K was obtained by Lebedev et al. [21] from EMF measurement. Yassin and Castanet [32] collected the partial enthalpy data of the Sm–Sn system from these literatures [21,28–31], and proposed a linear dependence on temperature for these selected data sets.

Additionally, Percheron et al. [29] measured the enthalpies of formation of the $SmSn_3$, Sm_2Sn_3 and Sm_5Sn_3 compounds at 295 K by liquid metal solution calorimetry. Using different techniques, the standard enthalpies of formation of the $SmSn_3$ and Sm_5Sn_3 phases were re-determined by Palenzona et al. [33] and Meschel and Kleppa [34], respectively. Colinet and Pasturel [35] predicted the enthalpies of formation of the intermetallic compounds in the Sm–Sn system with Miedma's model and Witusiewicz et al. [36] also obtained the evaluated enthalpy values based on the regularities of lanthanide compounds. The integral enthalpies of formation of the liquid Sm–Sn alloys at 1203 K were measured in the Sn-rich side ($0 < x(Sm) < 32$ at%) by Berrada et al. [37], who also estimated the limiting partial enthalpy of mixing of Sm in liquid Sn at 1203 K.